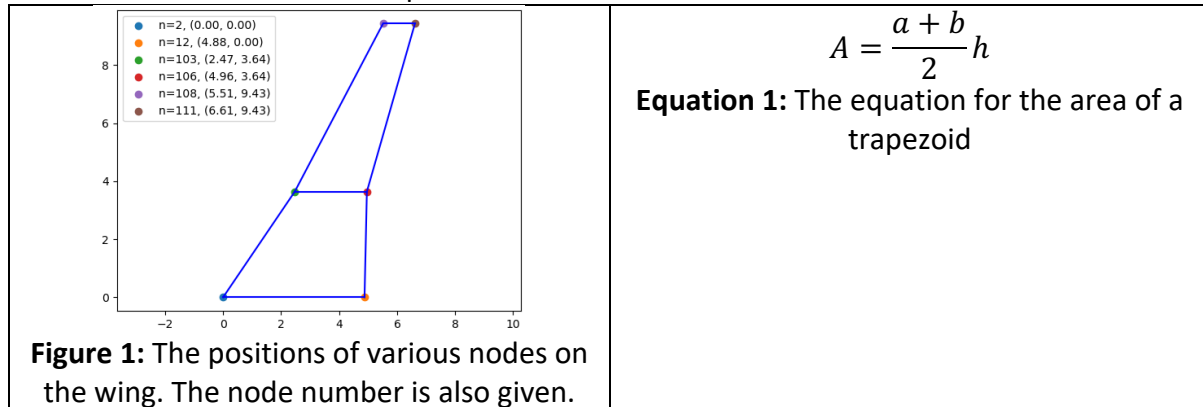


## Section 1

Using the position of various nodes, as given in Figure 1, the area of the wing could be found using Equation 1. This resulted in a wing area of  $23.78m^2$ , and from this, the loading could be calculated. These loads are presented in Table 1.



	Lift force = $F_z$	Drag force = $F_x$
Wing Up	122363N	7283.6N
Wing down	-43701.3N	2913.4N

**Table 1:** Loads for different conditions

In ANSYS, the SHELL181 element type was selected for the ribs, the spars and the skin. The choice of SHELL181 is obvious for the skin, as they can be curved, a necessary feature for an airfoil. As requested, the load is applied at the tip of the wing, meaning that there are no forces normal to the shells. This is ideal, as the shell elements should not be used for calculating normal forces. Beam elements could have been used, however the ribs and spars do not have a constant cross section.

A thickness of 0.015m was used for the shells, as this prevented yielding and gave a safety factor of roughly 1.8. This is in line with industry standards.

For each kind of boundary condition, the constraints were applied on the lines at the root of the wing. This was done instead of applying the constraints on keypoints to minimise the risk of singularities. Additionally, when the constraints were applied to the keypoints, the skin between these keypoints appeared to buckle. Applying the constraints to the lines instead solved these issues.

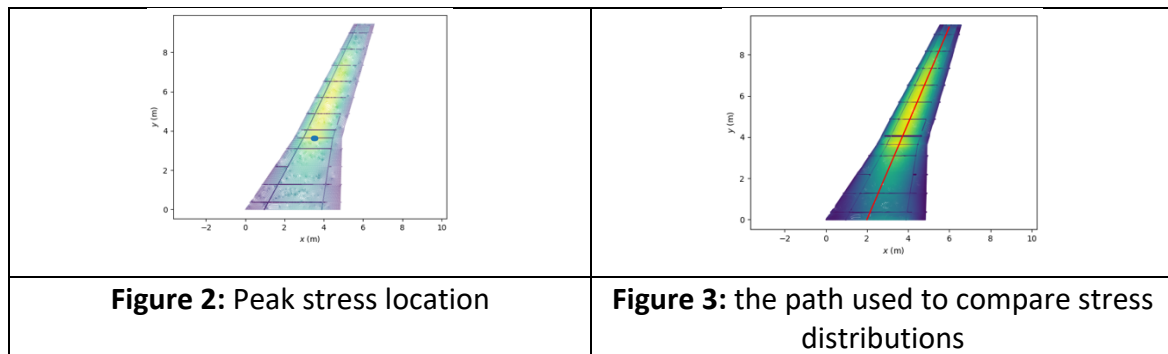
The loads were applied to the tip of the wing, as instructed. When applied to the keypoints, this caused a singularity. To get around this, the load was applied to the nodes instead. The loads were each identical, and were the values in Table 1, divided by the number of nodes. This was calculated using parameters to minimise the risk of operator error.

Applying the loads this way will have added more errors. Obviously, the forces over a wing act over the length of the wing, as opposed to just at the tip. Because the wing is swept, this

will lead to a higher angle of twist than should be expected. If the deformed shape of the wing is used in a further CFD analysis, this will lead to lower lift than would be expected. Additionally, the distribution of lift and drag was constant over the tip of the wing. This is also unrealistic, as lift distributions are not constant over a real wing. This will likely mean that the twist of the wing will be affected. I assume that this effect is small compared to the other modelling error.

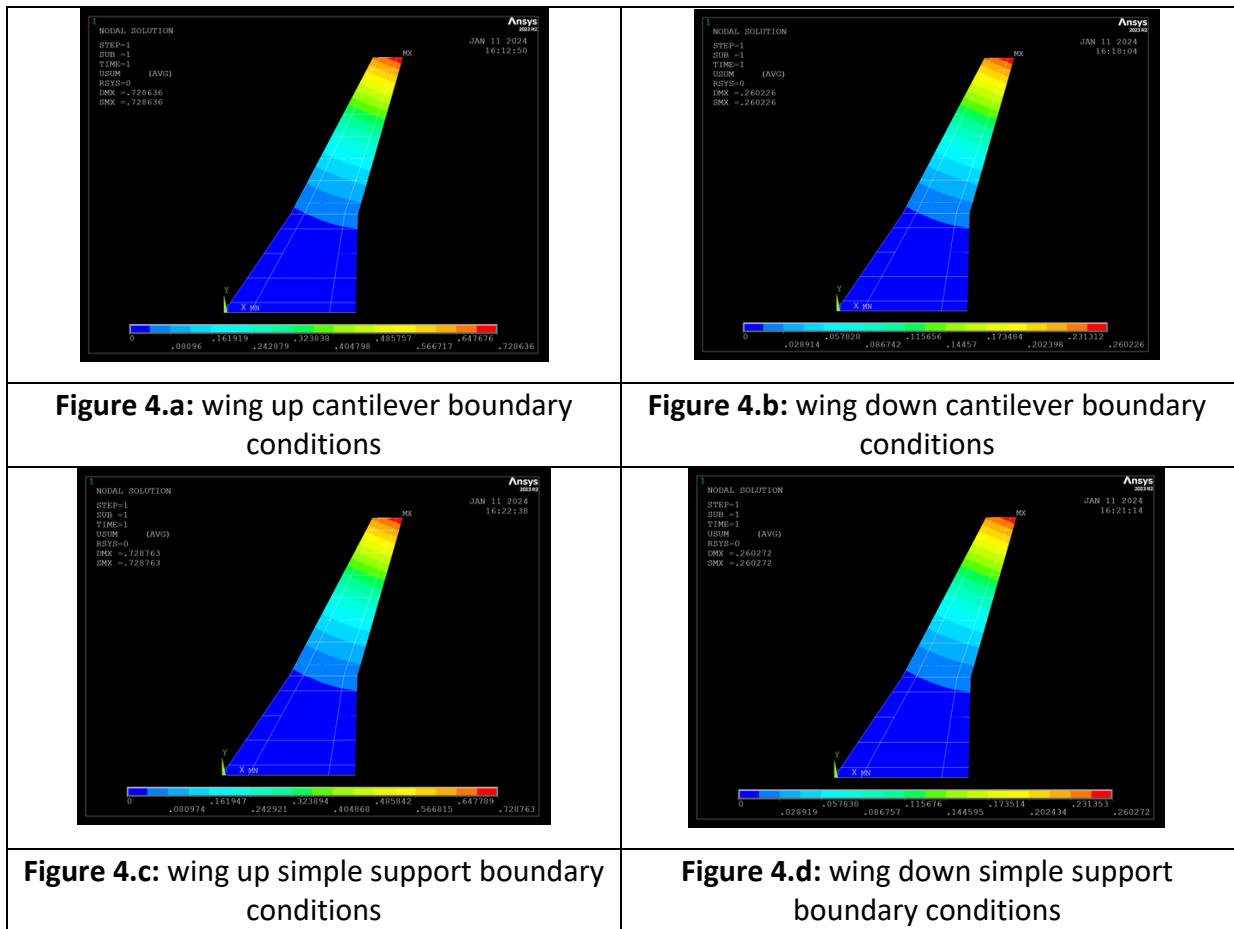
Another possible source of error will be that it appears that a section of a rib is missing. This is visible in Figure 2, near  $y = 2$ . The peak stress is around  $y = 3.46$ , notably where the geometry changes (see nodes 103, 106 in Figure 1). This leads me to believe that the impact of the missing spar is minimal, however it does seem noteworthy that it occurs near the same point as a change in geometry. The location of peak stress was found through sorting all nodes based on their value of Von Mises stress in python, and simply extracting the  $y$  coordinate of the first node. Visually, this makes sense.

Figure 3 shows the path used to generate the stress distributions. It goes from  $(2,0)$  to  $(6,9.34)$  with all of these units being in meters. The distributions were generated by exporting node positions, stresses and displacements from ANSYS, and using a custom solution to generate the path plots. The software used to generate these is available on request.



The boundary conditions used were all degrees of freedom fixed, the cantilever boundary condition, and displacements fixed with free rotation, the simple support boundary condition. The results for the vector sum of displacement is shown in Figure 4.

As well as this, the simple support gives rise to marginally more displacement. The reason this is so low, is that the moments at the wing are small, and the overall bending moment is distributed above and below the  $x$  axis, and it is mostly resisted by tensile and compressive loading.



For both wing up and wing down loading, the simple support gives more displacement than the cantilever support. This is expected, because less of the wing is constrained. As explained above, the additional displacement is marginal.

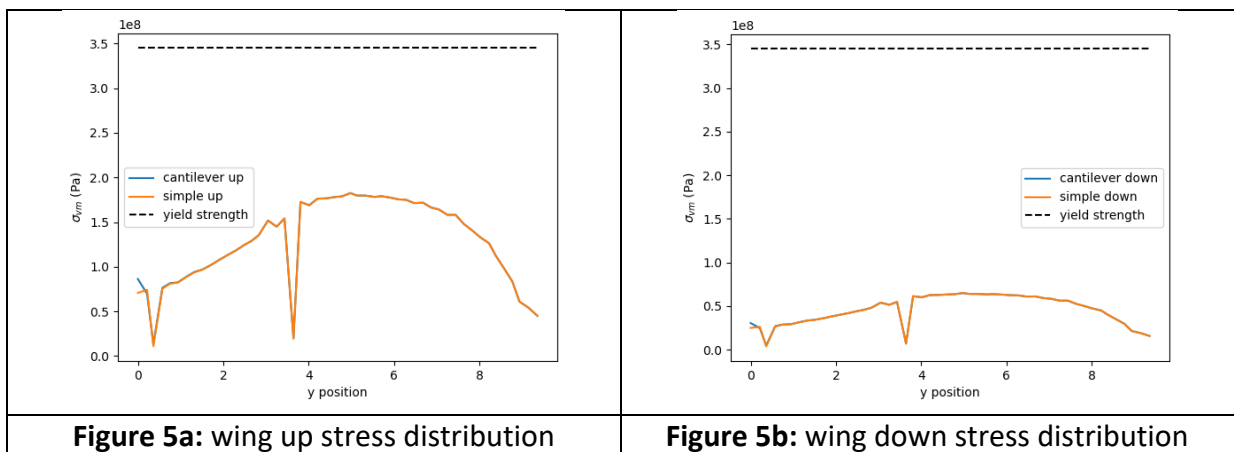


Figure 5 demonstrates the distribution of stress along the wing. The dips on the graph are ribs. Note that despite the units being pascals, the numbers on the y axis are to the power

of 8. The safety factor for the highest loading is around 1.8, which is in line with industry standards.

## Section 2

Mesh size	Element type	Element size (m)	No. Elements	No. Nodes
Coarse	SHELL181	0.1	7013	6498
Medium	SHELL181	0.05	25176	24178
Fine	SHELL181	0.01	646544	641630

When using the fine mesh, there was a lot more computational time expended. Looking at task manager while this was ongoing, it shows that this was due to high hard drive usage. In an enterprise setting, this would be solved by keeping the database on an SSD, however the computer used did not have enough spare SSD space. This additional time meant that it was harder to rapidly iterate, but it was possible to set the solve running and process the results later, while staying busy with other work.

While the maximum stress values in Figure 7 may indicate that the mesh affected the results, as the medium mesh has a dramatically lower value than the other meshes, Figure 6 shows the reason for this. The rib causes a peak in the stress for the coarse and fine meshes, but a trough in stress for the medium and fine meshes. Other than this, the distributions are very similar. The corner of the rib and the skin would likely lead to a stress concentration in a real wing, so a fillet would be added. This would decrease the peak of the wing back in line with the other meshes.

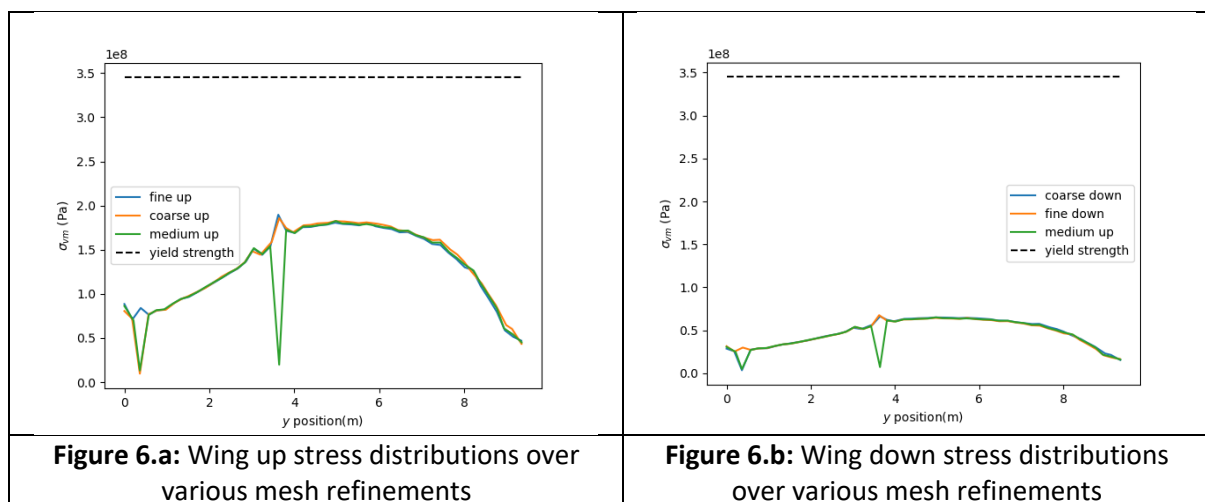


**Figure 6.a:** Wing up stress distributions over various mesh refinements

**Figure 6.b:** Wing down stress distributions over various mesh refinements

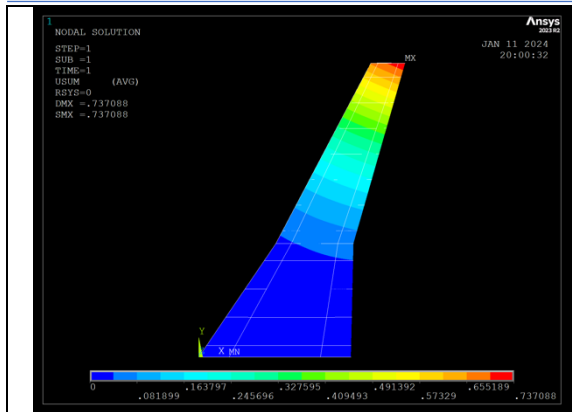


**Figure 7.a:** Displacement contours for wing up loading on a coarse mesh

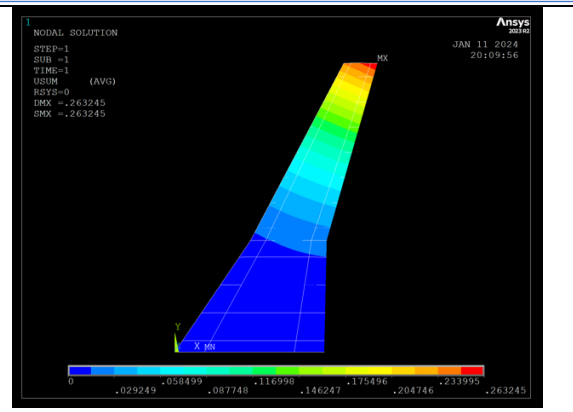


**Figure 7.b:** Displacement contours for wing down loading on a coarse mesh

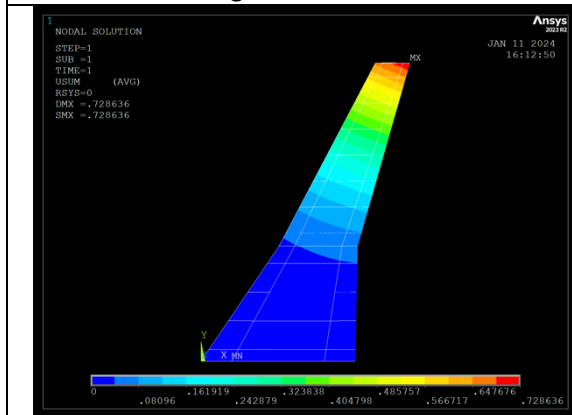


**Figure 7.c:** Displacement contours for wing up loading on a medium mesh

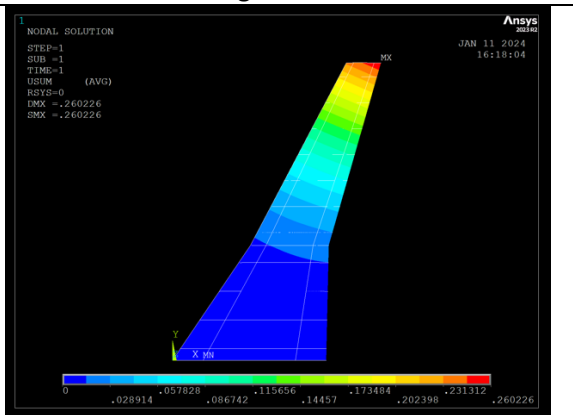


**Figure 7.d:** Displacement contours for wing down loading on a medium mesh

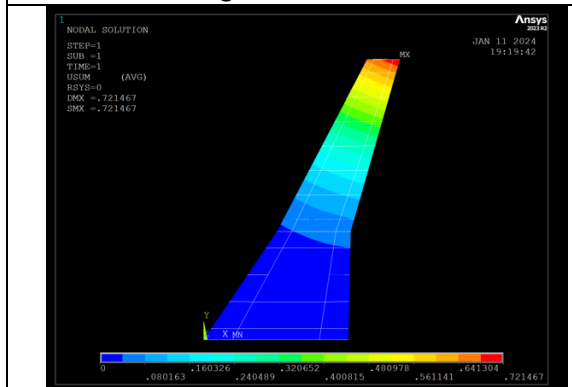


**Figure 7.e:** Displacement contours for wing up loading on a fine mesh

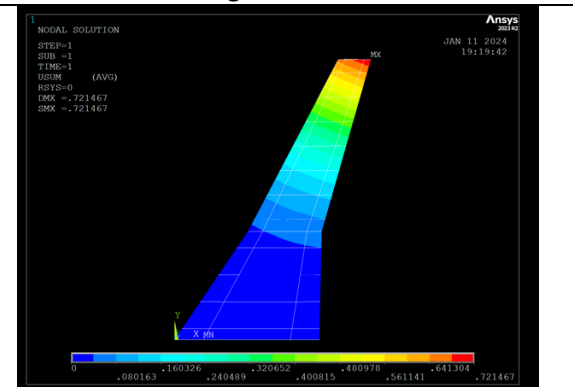


**Figure 7.f:** Displacement contours for wing down loading on a fine mesh

Seeing as the stress distributions are incredibly similar for all of the meshes, I think that it is clear that the solution is mesh independent. This does not imply that the solution shown is the solution a real wing would show. As discussed in Section 1, there appear to be some modelling errors which will affect the solution. In addition to this, any solution that APDL will produce will be the solution to a discretized version of a real problem. This introduces additional errors, as real parts are continuous, rather than discrete.

On hardware manufactured within the past 10 years, there will be no noticeable increase in speed by using the coarse mesh rather than the medium mesh. Additional memory may be used, but this is once again negligible.

For the fine mesh, the number of elements dramatically increased. This naturally lead to an increase in numbers of degrees of freedom. As the computational time scales with the number of degrees of freedom squared, this dramatically increased computational time to around 10 minutes per solution. While the solution was running, windows' task manager showed that hard drive use was at 100%, however transfer rates were in the single digits of megabytes. This suggests that APDL's solver could be optimized, however this does not appear possible for a user to solve.

Because all of the meshes have essentially the same results, the only value that matters is computational effort. For this, either the medium or coarse mesh could be used.

The medium mesh will be selected, because this allows for more accurate simulations of curves with linear elements, as are used here. This is important, because the wing is obviously curved. To approximate this with linear elements, many small elements are needed. If the curve is not well approximated, this will lead to excess shear stress on some nodes.

Type	Number of nodes	Number of elements
linear	24178	25176
quadratic	73779	25276

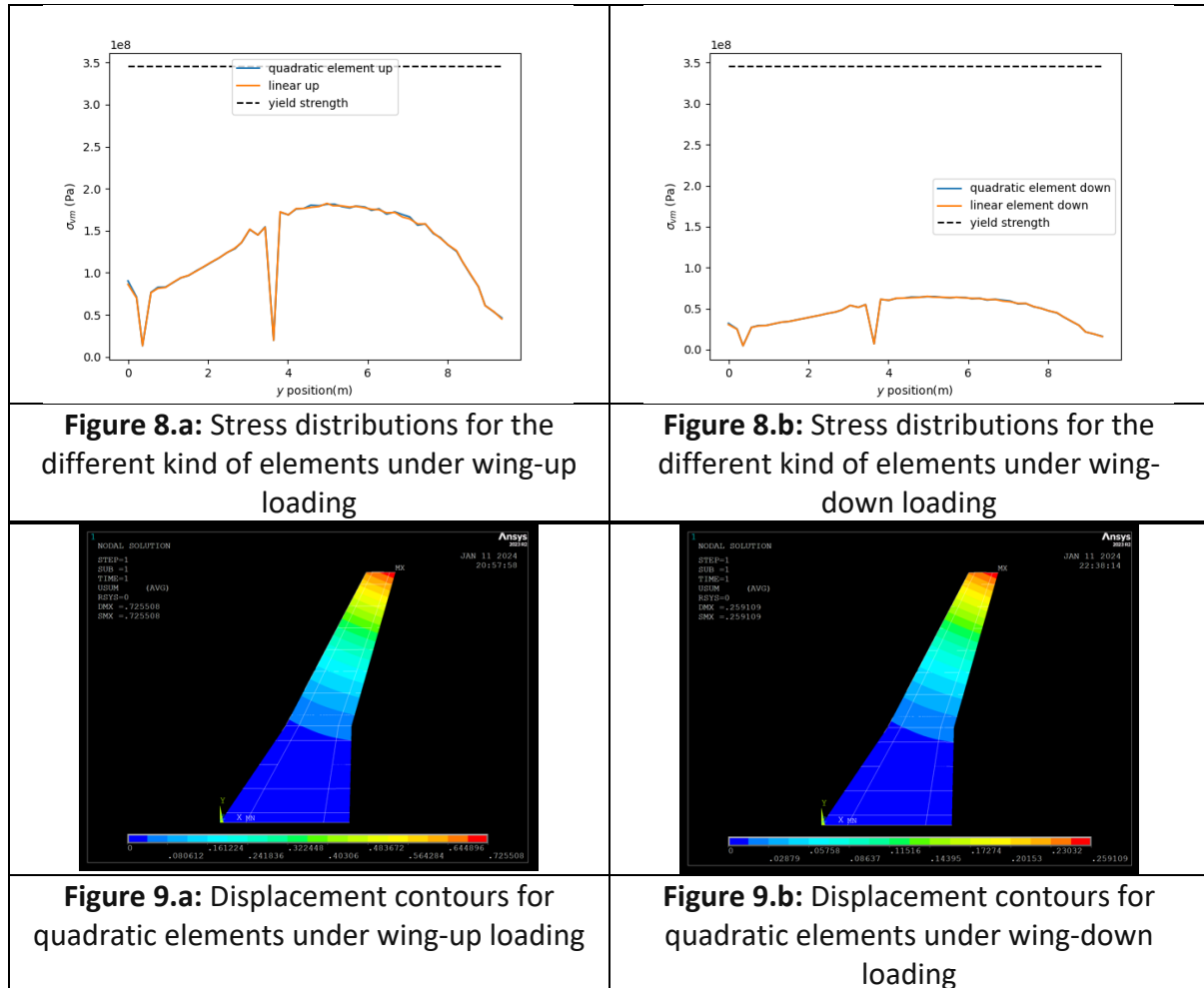
## Section 3

Figure 9 shows the displacement contours for the quadratic elements. For the displacement contours of the linear elements, see Figures 7b,c.

The additional degrees of freedom lead to an increase of the solution time from negligible to roughly 10 seconds. This is still fast enough to rapidly iterate and is not a concern. This further justifies the use of the medium mesh rather than the fine mesh. The medium mesh would likely take on the order of half an hour per solution, meaning a full hour just for both loading conditions, never mind the six additional runs for material selection.

While the stress distribution is clearly very close to the same, the quadratic elements will lead to slightly higher accuracy. This result suggests that the mesh size used is adequate to capture the curved shape of the wing with linear elements.

Because stress models are needed for this work, the additional accuracy is worth the marginal increase in time, so quadratic elements will be used.



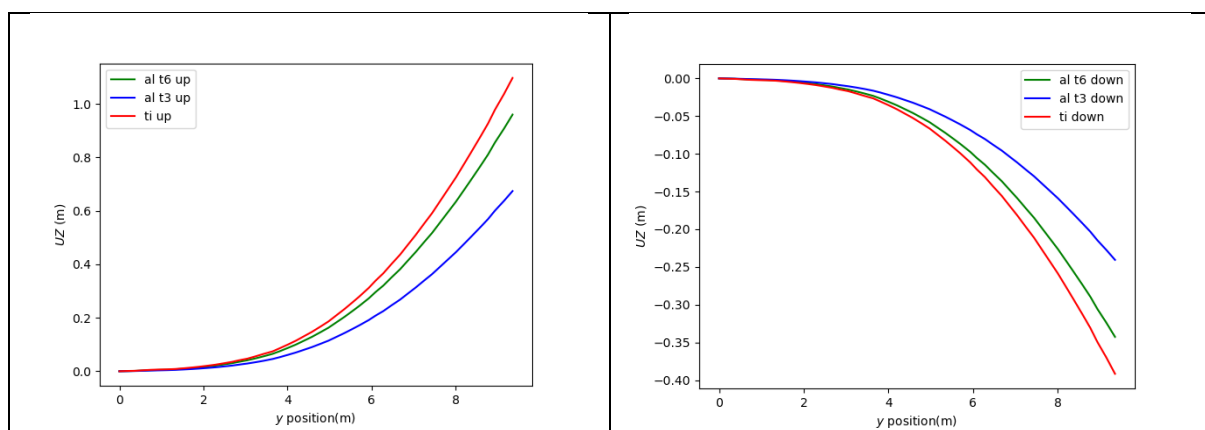
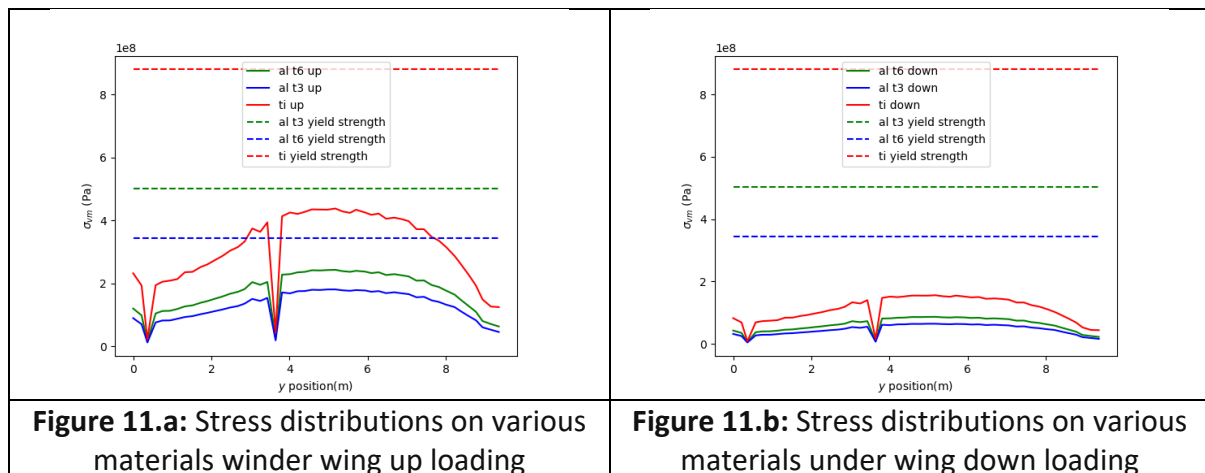
## Section 4

Unsurprisingly, changing the material choice will affect the safety factor of a structure. For this reason, all of the wings have had thicknesses adjusted so that the safety factor is approximately 1.8.

Because titanium has a significantly higher yield stress than the other materials, this means that the stress is naturally higher at any given point. The same is true of 7075-T6 when compared to 2024-T3. This is evident in Figure 11. The vertical displacements are shown in Figure 12. This appears to be correct, because more work must be done deforming the structure for the wing to be in equilibrium. The order of the curves agrees with this, as they are in the same order as Figure 11.

Table 2 lists the costs of the wings, assuming that the manufacturing processes are fully efficient. There will obviously be waste in the manufacturing process, so this is only an first-pass estimate. Additionally, this does not account for the cost to manufacture the wing, only the material used. Obviously, processing must be done to turn  $0.854m^3$  of 2024-T3 into a functional wing. The cost clearly rules out the titanium, except from very specific use cases such as aircraft where no price can be put on weight, however the ultimate cost of a 7075-T6 wing may be higher, due to factors such as dimensions of stock material, manufacturability and ongoing maintenance costs. For these reason, the “cheaper” wing cannot be found purely through this analysis. However, the raw material cost of 7075-T6 aluminium is clearly the cheapest option.

<b>Table 2</b>	2024-T3	7075-T6	Ti-6Al-4V
Volume ( $m^3$ )	0.854235	0.626439	0.34169
Weight ( $kg$ )	2374	1760	1514
Cost (\$)	10,683	6,152	60,560







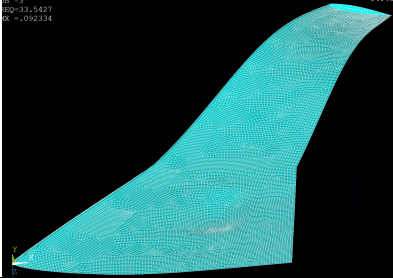
<b>Figure 12.a:</b> Vertical displacements for different materials experiencing wing up loading	<b>Figure 12.a:</b> Vertical displacements for different materials experiencing wing down loading
---	---

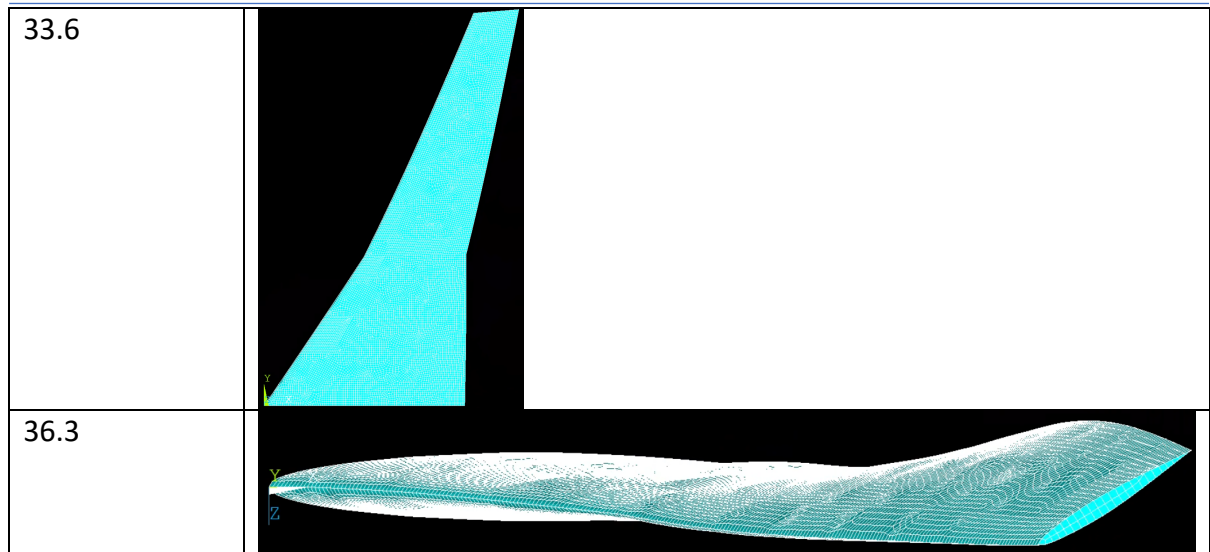
## Section 5

Static analysis is essentially loading at a frequency of 0. Modal analysis changes this by changing the frequency of the applied load.

Generally, the longer the characteristic length of the vibration, the lower the natural frequency of vibration.

Different natural frequencies excite different combinations of degrees of freedom. For low frequencies, this will usually be one degree of freedom, but for higher frequencies and therefore mode numbers, this can mean exciting multiple degrees of freedom at once. Modal analysis allows for design work to be undertaken to shift the frequencies. This can be important if a mode shape's natural frequency is near the frequency of a short-period oscillation, as exciting one may excite the other, leading to a loss of control in the worst case, or unnecessary cyclic loading in the best case. It is clear from the table below that the geometry of the wing means that the second trapezoid is where most of the resonant modes lie.

$\omega$	Shape
4.4	
16.1	
33.5	



The mode at  $\omega = 33.6$  appears to have a weakness due to the missing rib. This may be an error in the model, and if so this mode would not exist in the real structure.